Magnesium therapy improves outcome in Streptococcus pneumoniae meningitis by altering pneumolysin pore formation

Hupp, Sabrina; Ribes, Sandra; Seele, Jana; Bischoff, Carolin; Förtsch, Christina; Maier, Elke; Benz, Roland; Mitchell, Timothy J; Nau, Roland; Iliev, Asparouh I

Document Version
Peer reviewed version

[Link to publication on Research at Birmingham portal](#)

Title: Magnesium therapy improves outcome in *Streptococcus pneumoniae* meningitis by altering pneumolysin pore formation

Running (short) title: Magnesium benefits pneumococcal meningitis

Authors: Sabrina Hupp[1,3]*, Sandra Ribes[2]*, Jana Seele[2]*, Carolin Bischoff[3], Christina Förtsch[3], Elke Maier[4], Roland Benz[4], Timothy J. Mitchell[5], Roland Nau[2], Asparouh I. Iliev[1,3§]

*These authors contributed equally

[1] Institute of Anatomy, University of Bern, Baltzerstrasse 2, 3012 Bern, Switzerland

[2] Department of Neuropathology, University Medical Center Göttingen, Robert Koch Str. 40, 37075 Göttingen, Germany, and Department of Geriatrics, Evangelisches Krankenhaus Göttingen-Weende, An der Lutter 24, 37075 Göttingen, Germany

[3] DFG Membrane/cytoskeleton Interaction Group, Institute of Pharmacology and Toxicology &

Rudolf Virchow Center for Experimental Medicine, University of Würzburg, Versbacherstr. 9, 97078 Würzburg, Germany

[4] Rudolf Virchow Center for Experimental Medicine, University of Würzburg, Versbacherstr. 9, 97078 Würzburg, Germany

[5] Chair of Microbial Infection and Immunity, Institute of Microbiology and Infection, College of Medical and Dental Sciences, University of Birmingham, Edgbaston, Birmingham B15 2TT, UK

Conflict of interest statement: authors declare no conflict of interest.

Author contribution: experimental design –AI, RN, RB; performed experiments – SH, SR, JS, CB, CF, EM, AI, RN; analysed data - SH, SR, JS, EM; wrote manuscript - SH, SR, JS, AI, RN, RB, TM; provided materials – TM.

§ To whom correspondence should be addressed: Asparouh I. Iliev, MD, PhD, Institute of Anatomy, University of Bern, Baltzerstrasse 2, 3012 Bern, Switzerland, e-mail: asparouh.iliev@ana.unibe.ch; Tel: +41 31 631 3887, fax: +41 31 631 3807.

Abstract

Background and purpose. *Streptococcus pneumoniae* is the most common cause of bacterial meningitis in adults and is characterised by high lethality and substantial cognitive disabilities in survivors. Here, we study the capacity of an established therapeutic agent, magnesium, to improve survival in pneumococcal meningitis by modulating the neurological effects of the major pneumococcal pathogenic factor pneumolysin.

Experimental approach. We used mixed primary glial and acute brain slice cultures, pneumolysin injection in infant rats, a mouse meningitis model, and complementary approaches such as Western blot, a black lipid bilayer conductance assay and live imaging of primary glial cells.

Key results. Treatment with therapeutic concentrations of magnesium chloride (500 mg/kg in animals and 2 mM in cultures) prevented pneumolysin-induced brain swelling and tissue remodelling both in brain slices and in animal models. In contrast to other divalent ions, which diminish the membrane binding of pneumolysin in non-therapeutic concentrations, magnesium delayed toxin-driven pore formation without affecting its membrane binding or the conductance profile of its pores. Finally, magnesium prolonged the survival and improved clinical condition of mice with pneumococcal meningitis in the absence of antibiotic treatment.

Conclusions and implications. Magnesium is a well-established and safe therapeutic agent that has demonstrated capacity for attenuating pneumolysin-triggered pathogenic effects on the brain. The improved animal survival and clinical condition in the meningitis model points to magnesium as a promising candidate for adjunctive treatment of pneumococcal meningitis together with antibiotic therapy.

Non-standard abbreviations

CDC – cholesterol-dependent cytolysin

CFU – colony-forming unit

HU – haemolytic unit

LDH – lactate dehydrogenase

Mg – magnesium chloride, $MgCl_2$

PI – propidium iodide

PLY - pneumolysin

PSD95 – postsynaptic density 95

Introduction

Streptococcus pneumoniae (pneumococcus) is a common bacterial pathogen that causes meningitis in humans, accompanied by high lethality (~30%) and substantial cognitive disabilities in survivors (Koedel, Scheld & Pfister, 2002). Pneumolysin (PLY), a member of the cholesterol-dependent cytolysin (CDC) group and a major pneumococcal neurotoxin, is one of the key pathogenic factors that causes deterioration over the course of *S. pneumoniae* meningitis (Wellmer et al., 2002) and pneumococcal lung infections (Canvin et al., 1995). PLY produces pores and cell lysis at high concentrations and non-lytic changes at lower concentrations (Iliev, Djannatian, Nau, Mitchell & Wouters, 2007a; Iliev et al., 2009). The CDC protein family includes toxins from Gram-positive bacteria that share a common dependence on the presence of cholesterol in cell membranes (Alouf, 2000). PLY-expressing pneumococcal strains cause more severe disease than PLY-negative strains (Reiß et al., 2011), and the concentration of PLY in the CSF of patients with meningitis correlates with the outcome (Wall et al., 2012).

PLY, which has been thoroughly studied ultrastructurally in artificial membranes (Tilley, Orlova, Gilbert, Andrew & Saibil, 2005), produces pores by first binding to membrane cholesterol, aligning in arcs and forming pre-pore structures of 30-50 monomers, followed by molecular unfolding and membrane perforation producing 26-30 nm wide lytic pores. The toxin comprises 4 domains: domain 4 mediates binding to membrane cholesterol, while domains 1, 2 and 3 establish the pre-pore barrel. Upon alignment in a ring-shaped pre-pore, domain 3 refolds into two β hairpins (each containing two parallel β-strands), which penetrate the membrane and build the internal β-barrel of the pore (Tilley, Orlova, Gilbert, Andrew & Saibil, 2005). The artificial membrane ultrastructural studies utilise mostly concentrations of 2 µg/ml PLY and higher. In the CSF of patients with meningitis, however, the concentrations of PLY do not exceed 0.2 µg/ml, which is mildly lytic in cell cultures and non-lytic in tissue culture systems (Iliev, Djannatian, Nau, Mitchell & Wouters, 2007a; Iliev et al., 2009; Spreer et al., 2003). We shall call such concentrations sublytic. We have shown before that sublytic concentrations of PLY produce cytoskeletal changes, including actin remodelling and microtubule stabilisation, without plasmalemmal permeabilisation (Iliev, Djannatian, Nau, Mitchell & Wouters, 2007a; Iliev et al., 2009). The short-term (within a few hours) effects of PLY involve interstitial tissue oedema and increased pathogen tissue penetration in the brain, both caused by astrocyte remodelling (Hupp et al., 2012).

The management of bacterial meningitis involves corticosteroids as adjuvants to prevent fatal oedema (Grandgirard & Leib, 2010) and includes antibiotics. The administration

of bactericidal non-bacteriolytic antibiotics has proven to reduce lethality and sequelae more effectively than bacteriolytic antibacterials, most likely due to the reduced concomitant release of neurotoxic factors such as PLY (Grandgirard, Burri, Agyeman & Leib, 2012; Nau et al., 1999; Spreer et al., 2003). However, the bacteriolytic family of β-lactam antibiotics still constitutes the standard treatment, and no efficient and clinically applicable therapy exists to counteract the detrimental effects of PLY already released into the central nervous compartments.

In this work, we demonstrate that clinically relevant doses of magnesium (Mg) diminish most of the tissue pathogenic effects of PLY and improve the outcome of pneumococcal meningitis in animal models of the disease.

Methods

Pneumolysin preparation

Wild-type PLY was expressed in *Escherichia coli* BL-21 cells (Stratagene, Cambridge, UK) and purified by metal affinity chromatography as described previously (Douce, Ross, Cowan, Ma & Mitchell, 2010). The purified PLY was evaluated for the presence of contaminating Gram-negative LPS using the colorimetric LAL assay (KQCL-BioWhittaker, Lonza, Basel, Switzerland). All purified proteins showed <0.6 endotoxin units/µg of protein. The stock of purified wild-type toxin exhibited an activity of 2 x 10^4 haemolytic units (HU)/mg.

Cell and slice cultures, vital staining, live imaging and treatments

Primary glial cultures (astrocytes and microglia) were prepared from the brains of postnatal day (P) 4-6 of either C57BL/6 mice (Janvier Labs, Le Genest-Saint-Isle, France) or Sprague Dawley (SD) rats (Charles River WIGA GmbH, Germany) as previously described (Iliev, Stringaris, Nau & Neumann, 2004) in DMEM (Life Technologies, Thermo Fisher Scientific, Schwerte, Germany) supplemented with 10% foetal calf serum (FCS) (PAN Biotech GmbH, Aidenbach, Germany) and 1% penicillin/streptomycin (Life Technologies) in 75 cm^2 poly-L-ornithine- (Sigma-Aldrich Chemie GmbH, Schnelldorf, Germany)-coated cell culture flasks (Sarstedt AG & Co., Nuembrecht, Germany). The total number of animals used for primary cultures was 10, they were sacrificed by decapitation (an approved method in the German Animal Protection Law (Tierschutzgesetz)).

Acute brain slices were prepared from P10-14 C57BL/6 mice (12 animals) or SD rats (12 animals) by decapitation. It allows to obtain brain tissue in optimal condition for acute brain slices by vibratome sectioning (Vibroslice NVSL, World Precision Instruments, Berlin, Germany) in BME continuously oxygenated with carbogen gas (95% O_2, 5% CO_2) at 4°C. The slices were allowed to adapt in carbogenated BME (Life Technologies) medium with 1% penicillin/streptavidin and 1% glucose at 37°C for 1 h before being challenged with PLY under the same conditions. In these acute slices, cell lysis never exceeded 5% within 12 h (as judged by a lactate dehydrogenase (LDH) release test).

In tissue remodelling experiments, the acute slices were incubated with 70-kD dextran-TRITC (Life Technologies, 0.5 mg/ml) for 10 min at 37°C before fixation with 2% paraformaldehyde (Carl Roth GmbH, Karlsruhe, Germany) in PBS to assess molecular penetration. The fixed samples were examined by scanning confocal microscopy on a Leica LSM SP5 (Leica Microsystems Heidelberg GmbH, Mannheim, Germany) followed by 3D

reconstruction of the z-stacks (1-µm scanning step) and measurement of penetration using ImageJ software (version 1.43g for Windows OS, National Institute of Health, Bethesda, Maryland, USA).

For live imaging experiments, the cells were incubated at 37°C in CO_2-insensitive L-15 Leibovitz`s medium (Life Technologies) containing propidium iodide to stain permeabilised cells, and Hoechst 33342 to stain the nuclei of all cells (1 µg/ml, Life Technologies). The cells were visualised on an Olympus Cell-M Imaging system using the 10x and 20x dry objectives (Olympus Deutschland GmbH, Hamburg, Germany).

Lactate dehydrogenase (LDH) release assays were performed using CytoTox96 non-radioactive cytotoxicity assay according to manufacturer`s instructions (Promega, Madison, WI, USA).

In all experiments, cells and tissues were treated with PLY in serum-free medium. Magnesium chloride hexahydrate was purchased from Merck Millipore (catalogue number: 105833) and dissolved in 0.45% saline. Calcium chloride was purchased from Sigma.

Animal procedures and choice of animal models

All animal experiments were performed according to the regulations of the German Research Animal Protection Law (Tierschutzgesetz) with approval from the Commission for Animal Experiments Government of Lower Franconia, Bavaria, Germany, and approval from the Authority for Consumer Protection and Food Safety of Lower Saxony (Niedersächsisches Landesamt für Verbraucherschutz und Lebensmittelsicherheit (LAVES)), Braunschweig, Lower Saxony, Germany, Germany. All animals were maintained for one week before the start of the experiments in an animal facility with 12/12 h light/dark cycles and water and food ad libitum. All experiments were terminated in such a way as to avoid animal suffering. Animal experiments were performed in two different animal species systems (mice and rats) to increase cross-species translational relevance. The choice of the most suitable animal model for experiments represents a major task that has to be considered carefully. Ample evidence indicates the risk of misleading interpretations when using only one species model or model that is not at correct age, correct condition or susceptible to disease (Denayer, Stöhr, & Van Roy, 2014). The most widely used experimental animal model species are rats and mice and despite being wrongly considered similar, they are actually separated by 12-24 million years of evolution and differ substantially (Blanga-Kanfi et al., 2009). Thus, verification of therapeutic effect simultaneously in both species increases substantially the chance of translational value to humans. At the same time, the current legal and bioethical

standpoint strongly urges researchers to reduce the number of experimental animals, especially when experimental models are accompanied with potentially higher level of suffering (Flecknell, 2002). To accommodate both issues, we chose to verify the effects of magnesium in two live animal models – Sprague-Dawley rats and C57Bl/6 mice, testing the role of magnesium on pure toxin in one of them only and the effect in full-scale disease in the other.

For induction of PLY-based animal brain swelling, 29 infant SD rats (P10-14) were used. The choice of the model was based on our earlier experience that showed more efficient intracerebroventricular (icv) toxin distribution in the ventricular system of rats versus mice when toxin-induced swelling was studied (Hupp et al., 2012). Rats were randomly distributed in the following groups: icv saline-injected mock control (n=9), icv PLY-injected group (n=11), and Mg (500 mg/kg) pre-treated and subsequently icv PLY-injected group (n=9). The animals were anaesthetised with ketamine/xylazine (sc, ketamine, 80 mg/kg; xylazine, 12 mg/kg; Sigma), with follow-up anaesthesia using ketamine (sc, 30 mg/kg/h). During the experiments, the blood pressure and the pulse frequency of each anaesthetised animal were monitored by a non-invasive tail measurement system (Stoelting Co., Wood Dale, IL, USA) to confirm proper physiological conditions. To verify the pathophysiological relevance of the injected amounts, samples from the CSF were taken within 2 h of the injection of PLY and/or 1% Evans Blue dye (Sigma) to confirm the complete distribution of the injected fluid in the CSF. The final concentration of PLY was 0.2 µg/ml (Wippel et al., 2011), which was comparable to the toxin amounts observed in the CSF during pneumococcal meningitis (Spreer et al., 2003). Equimolar amounts of albumin Fr. V (Sigma) were applied instead of PLY in control animals.

For induction of bacterial meningitis, 44 two-month-old female C57BL/6 mice were used according to an established protocol, used repetitively in the field (Nau et al., 1999). Mice received an intracerebral (ic) injection of either 10 µl containing 1×10^5 CFU/ml (1 000 CFU/mouse) of *S. pneumoniae* D39 in saline (n=37) or 10 µl of sterile saline (n=7) after intraperitoneal (ip) anaesthesia with ketamine (100 mg/kg) and xylazine (10 mg/kg) (Wellmer et al., 2002). The health status of the mice was assessed every 12 h by a clinical score [0, no apparent behavioural abnormality; 1, moderate lethargy (apparent decrease of spontaneous activity); 2, severe lethargy (rare spontaneous movements, but walking after stimulation by the investigator); 3, unable to walk; 4, dead] (Gerber et al., 2001), and the areas under the curves (AUCs) of the clinical scores were calculated for each animal. As a consequence of the muscle-relaxant effect of Mg, animals receiving $MgCl_2$ were susceptible

to an inhibition of ventilation by anaesthetics. To avoid negative potentiation of ventilation inhibition, $MgCl_2$ administration was delayed with 30 min after introduction to anaesthesia. To limit the number of injections, animals were treated with 3 doses (every 12 h, starting 30 min before ic injection) of a 0.33 ml solution containing either 30.45 mg $MgCl_2$/ml or 0.33 ml of 0.45% saline intraperitoneally. Animals were treated ip with 0.33 ml solution of 30.45 mg $MgCl_2$/ml or 0.33 ml of 0.45% saline. Magnesium chloride hexahydrate was dissolved in 0.45% saline. As the $MgCl_2$-dependent effect was only observed until 12 hours after the last $MgCl_2$ treatment, mice were sacrificed under anaesthesia 36 h after infection by cervical dislocation. This time point was also defined to reduce excessive suffering of the animals when reaching 50% lethality. Blood samples, spleen and cerebellum were collected, plated and cultured on blood agar. The cerebrum was fixed in 4% formalin, dehydrated and paraffin-embedded for further processing and analysis (cutting, immunohistochemistry).

Animal group sizes, randomization, blinding and normalization

The number of experimental animals used was kept to a minimum by statistical optimisation in accordance with the Altman`s nomogram (O'Hara, 2008). The exact number of animals in different groups is indicated either in the figure legends or in the Methods section. The total number of animals used in all experiments was 113 (107 in the experimental series, 3 for adjustment of the anaesthesia and 3 for preliminary analysis of optimal Mg concentration). All animals were randomized before treatment. In all animal experiments and in all further sample analyses, the animals/samples were blinded before evaluation and un-blinded upon statistical analysis. Normalization versus control groups (mock-treated and Mg-treated controls) was employed in histological analysis of postsynaptic fluorescence intensity to correct for intensity staining changes by Mg-treatment. The work is reported in line with the ARRIVE guidelines as requested in the Instructions to Authors of the journal.

Oedema evaluation

For the analysis of brain swelling, 10 µl of 1% Evans Blue dye was injected icv 6 h after the first injection (mock or PLY), and the needle was kept in place for an additional 30 min, completely sealing the tiny skull opening. Within this time, nearly all dye was redistributed in the CSF. As the intracranial pressure increased, larger amounts of the dye/CSF mix would leak out after needle removal to equilibrate the pressure. The dye was absorbed onto filter paper, and the size of the spot, which was proportional to the total

amount of fluid, was scanned and measured (in mm^2) with ImageJ. This method for edema evaluation proved superior to others when working with infant rodents (Hupp et al., 2012). During the whole procedure, all animals were maintained under anaesthesia without interruption and at the end were sacrificed by cervical dislocation.

The water content of the brain slices was analysed by specific gravity (also known as relative density) measurement in a Percoll (Sigma) density gradient (Tengvar, Forssen, Hultstrom, Olsson, Pertoft & Pettersson, 1982). The gradient ranged from 1.065 to 1.009 and was produced by dilution of isotonic Percoll in PBS (10:1 Percoll:10x PBS), thus creating 21 layers in increments of 0.0025. Oedematous tissue demonstrates a decreased relative density due to its increased water content, so it floats in a Percoll layer with a lower relative density.

Immunohistochemistry

For the immunohistochemical experiments, microtome slices from mouse brains embedded in paraffin were deparaffinised and rehydrated, and the antigen was unmasked using target retrieval solution (Dako Deutschland GmbH, Hamburg, Germany) at 95°C. The primary antibodies used were rabbit anti-PSD95 (1:500; Abcam, Cambridge, UK) and rabbit anti-active caspase-3 (1:250; RnD Systems, Bio-Techne AG, Zug, Switzerland), and the secondary antibodies were goat anti-rabbit tagged with FITC or Cy3 (1:200; Dianova GmbH, Hamburg, Germany). Isotype controls confirmed the specificity of the staining. The sample nuclei were stained with DAPI (4,6-diamidino-2-phenylindole dihydrochloride, 1 µg/ml in PBS; Life Technologies). All samples were preserved with the ProLong antifade reagent (Life Technologies).

Protein biochemistry

Equal number of cells (500 000 per a 60 mm Petri dish) were challenged either with PLY alone or in the presence of additional 2 mM Mg for 15 min at 37°C in serum-free medium. Cells were washed 3 times with ice-cold PBS before proceeding further. Total crude cell membranes were isolated as described before (Iliev, Djannatian, Nau, Mitchell & Wouters, 2007b). Shortly, cells were homogenized in buffer containing 10 mM Tris HCl (pH=7.4), 1 mM EDTA, 200 mM sucrose (all from Sigma–Aldrich) and protease inhibitor mix (Roche Diagnostics, Mannheim, Germany). The nuclei and cellular debris were removed by centrifugation at 900 x g for 10 min at 4°C. The resulting supernatant was centrifuged at 110 000 x g for 75 min at 4°C. Part of this supernatant was used for actin protein control samples for the Western blots. The crude membrane pellet was solubilized in buffer

containing 10 mM Tris HCl (pH=7.4), 1mM EDTA, 0.5% Triton X-100 and protease inhibitor mix) and boiled in Laemmli buffer at 95°C for 20 min.

Samples containing equal amounts of protein (BCA test, Thermo Fisher) were loaded on a nitrocellulose membrane (Schleicher & Schuell GmbH, Dassel, Germany) using a Novex® Tris-Glycine polyacrylamide gel system (Life Technologies). After semi-dry blotting, the membranes were blocked with 5% non-fat milk and incubated with rabbit anti-PLY antibody (Abcam Inc.; 1:400) and mouse anti-actin antibody (Sigma; 1:1 000) as a loading control. After incubation with a horseradish peroxidase-conjugated goat anti-mouse and goat anti-rabbit secondary antibodies (Dianova), the bands were visualised using an ECL kit (GE Healthcare, Munich, Germany).

Planar (black) lipid bilayer experiments

The planar lipid bilayer experiments were carried out as previously described (Benz, Janko, Boos & Lauger, 1978). Membranes were formed from a 1% (w/v) solution of oxidised cholesterol in n-decane (Sigma). This artificial lipid was used instead of diphytanoyl phosphatidylcholine because it facilitates the insertion of porin and PLY pores into the lipid bilayer (Benz, Ishii & Nakae, 1980). The toxin (0.5 μg/ml) was added to the aqueous phase after the membrane had turned black. The membrane current was measured with a pair of Ag/AgCl electrodes with salt bridges switched in series by a voltage source and a highly sensitive current amplifier (Keithley 427, Keithley Electronics, Garland, TX, USA) in a buffer containing 100 mM KCl, 10 mM HEPES and various concentrations of $MgCl_2$. The temperature was maintained at 20°C throughout the experiment.

Evaluation and statistics

Image processing and image analysis were performed using ImageJ software, version 1.43g for Windows. Statistical analyses were performed on GraphPad Prism 4.02 for Windows (GraphPad Software Inc., La Jolla, CA, USA). Statistical tests included the Mann-Whitney U-test (comparing two groups, varying one parameter at a time), one-way ANOVA with a Bonferroni post-test (comparing three or more groups, varying one parameter at a time) and the log-rank test to compare survival between two groups. When non-linear regression analysis was performed, one-phase exponential association was used. For all analyses, we considered values of $p<0.05$ as statistically significant and indicated them with asterisk throughout. All values in the graphs represent mean ± SEM.

Nomenclature of Targets and Ligands

Key protein targets and ligands in this article are hyperlinked to corresponding entries in http://www.guidetopharmacology.org, the common portal for data from the IUPHAR/BPS Guide to PHARMACOLOGY (Southan et al., 2016), and are permanently archived in the Concise Guide to PHARMACOLOGY 2015/16 (Alexander et al., 2015).

Results

Magnesium diminishes interstitial brain edema by pneumolysin

Interstitial brain oedema caused by PLY represents a tissue-specific toxin effect (Hupp et al., 2012). Here, brain swelling was quantified using the reduction of the relative density in an acute brain slice culture model system. We used concentrations of PLY corresponding to 4 haemolytic units (HU)/ml, which were non-lytic but produced oedema in slices (Hupp et al., 2012). First, the effects of therapeutic concentrations of Mg (0.5-2 mM) on PLY-induced tissue swelling were investigated. The basal medium in all experiments contained 2.5 mM Mg, and $MgCl_2$ was added to the basal medium to reach therapeutic concentrations. In all experiments, the notation "without Mg" means without extra Mg above the basal medium concentration of 2.5 mM. Addition of 2 mM Mg completely blocked the brain oedema produced after 6 h of 4 HU/ml PLY exposure (Fig. 1A). Mg-induced prevention of brain swelling was concentration-dependent (Fig. 1B). Because PLY allows deeper penetration of whole pneumococci and bacterial products into the tissue due to wider intercellular spaces (Hupp et al., 2012), we quantified penetration using a fluorescently labelled dextran (MW=70 kD) incubation approach. Again, the addition of 2 mM Mg fully restored the normal permeability of the tissue when applied simultaneously with PLY and diminished the penetration of dextran to control values (Fig. 1C).

Next, we tested whether the beneficial effects of Mg were due to i) tissue conditioning, ii) modulation of the interaction of the toxin with the tissue, or iii) the effect on the toxin alone. First, slices were pre-incubated with high doses of Mg for 1 h before the toxin was added to the medium (PLY+Mg) (Fig. 2A). Tissue swelling was completely prevented. Next, we exposed slices to PLY and Mg without tissue pre-treatment with Mg (PLY & Mg). The beneficial effect of Mg was preserved again (Fig. 2A). In the third approach, slices were pre-challenged with Mg for 1 h, then Mg was removed and PLY added (group Mg→PLY). Here, Mg was ineffective against PLY-induced brain oedema (Fig. 2A). Altogether, this demonstrated that the action of Mg was most prominent when applied on the tissue together with PLY and thus Mg exerted its effect by modulating toxin/cell interactions. Pre-incubation of the toxin together with high doses of Mg for 1 h followed by slice challenge in base medium without extra Mg was partially effective against toxin-induced oedema (Fig. 2B), indicating some effect limited to the toxin only.

Magnesium diminishes the pore-forming capacity of pneumolysin

To analyse whether the elevation of Mg in the medium affects the binding of PLY to the cell membrane, we performed Western blot analysis on the membrane fraction from glial cells after challenge with PLY. No decrease in the toxin binding in primary glial cells was observed 15 min after challenge (Fig. 3A). Next, we measured the conductance of the PLY pores in black lipid membranes in the presence or absence of Mg to detect alterations in pore structure. No change in the conductance profile was observed in the conductance event frequency histograms with similar peak conductance around 25 nS (Fig. 3B). We studied the permeabilisation of primary glia in culture by PLY in the presence and absence of additional Mg. The concentrations that are pro-oedematous and non-lytic in slices are partially lytic in dissociated primary glial cultures (up to 10%, we call them sublytic), and this can be analysed by propidium iodide (PI) permeabilisation. Additional Mg significantly delayed the permeabilisation of glial cells by PLY (Fig. 3C, D) with differences in the permeabilisation endpoints after regression analysis curve extrapolation as well (Fig. 3E). LDH release cytotoxicity assay confirmed these findings. 5 h after toxin challenge in cell culture, however, the cytotoxicity of toxin challenged groups (both with and without additional Mg) equalized (Fig. 3F). Thus, Mg delayed pore formation by PLY without modulation of binding and conductance profile of the pores. All experiments were repeated both in SD rats and C57BL/6 mouse cell systems with similar outcomes.

Inhibition of brain swelling by pneumolysin in animals

Next, we tested whether the systemic application of Mg may be a suitable therapeutic alternative in whole-animal paradigms. We tested two different species systems to increase the translational relevance of our findings. Icv injection of PLY (at a final concentration of 4 HU/ml) into the CSF of young rats (P10-14) produced brain oedema as evaluated by the Evans blue method, following an established protocol (Hupp et al., 2012). Mg pre-treatment (500 mg/kg ip; dose was determined by extrapolation of the results from brain slices experiments to animals considering volume of distribution, effects of serum Mg elevation on CSF Mg concentration and preliminary tests in single animals) significantly reduced the amount of brain swelling in the infant rats 6 h after toxin challenge (Fig. 4). Mg demonstrated some muscle relaxation in treated animals under anaesthesia as determined by decreased muscle tonus.

Improved survival, synaptic loss and clinical status in meningitis animals

Finally, we investigated the role of Mg as a potential treatment in the mouse model of pneumococcal meningitis that has been widely used in the field (Nau et al., 1999). No differences in bacterial titers in spleen, cerebellum and blood (Fig. 5A) and in weight loss (Supplementary Fig. S1A) were observed between mock and Mg-treated infected animals at the end of the experiment. The predefined endpoint for analysis of lethality was 36 h (see Methods). Immunohistochemically, we analysed synapses in layers I-III of the neocortex by PSD95 (postsynaptic density 95 – a postsynaptic marker) immunostaining. The analysis revealed that Mg treatment blocked the loss of PSD95 immunostaining at 36 h after infection with *S. pneumonie* (Fig. 5B). No significant differences in the elevated number of cells positive for active caspase-3 in the CA2 area of the hippocampal formation were observed between the two groups of infected mice (Supplementary Fig. S1B). Mice receiving $MgCl_2$ had less severe clinical symptoms, i.e., a lower clinical score, than infected mock animals (Fig. 5C). Mg treatment prolonged the survival of mice with pneumococcal meningitis significantly (Fig. 5D). While in the group with mock-treated animals, 8 (out of 19) succumbed to the infection in the first 36h after infection**,** only 2 (out of 18) Mg-treated died before the endpoint.

Discussion

Our work demonstrates for the first time that clinically relevant concentrations of Mg, a well-known and established therapeutic agent, can prevent the brain pathogenicity of the neurotoxin PLY, which is released from *S. pneumoniae,* and provide a benefit for the outcome in animal models of pneumococcal meningitis.

Brain swelling, a complication of brain trauma, ischaemia, brain tumours and a variety of other disease conditions, contributes to lethality by compromising cerebral blood flow and/or by displacing important brain structures within the fixed volume of the skull (Marmarou, 2007; Raslan & Bhardwaj, 2007). The management of acute brain oedema in these cases is of primary clinical importance (Raslan & Bhardwaj, 2007). Brain swelling also plays a significant role in pneumococcal meningitis (Brandt, 2010; Kastenbauer & Pfister, 2003). Neuroinflammation and increased vascular permeability are considered major factors in infectious brain oedema (Stamatovic, Dimitrijevic, Keep & Andjelkovic, 2006). Earlier works have demonstrated that PLY can also produce intercellular oedema of the brain, widening the intercellular spaces and thus enhancing the tissue penetration of pathogenic factors and bacteria, as astrocyte reorganisation plays a key role in this process (Hupp et al., 2012).

The role of PLY as a critical pathogenic factor in pneumococcal meningitis has been verified in multiple experimental and clinical studies (Reiß et al., 2011; Wall et al., 2012; Wellmer et al., 2002). Lack of PLY is associated with much milder disease course and improved survival. Other members of the CDC toxin group such as perfringolysin and listeriolysin increase the virulence of their corresponding strains too (Awad, Ellemor, Boyd, Emmins & Rood, 2001; Bielecki, Youngman, Connelly & Portnoy, 1990; Jones & Portnoy, 1994). Immunisation with PLY improves the survival rates of mice infected intranasally with *S. pneumoniae* (Paton, Lock & Hansman, 1983). Similarly, neutralising antibodies against PLY improve the outcome after intranasal infection with *S. pneumoniae* and in PLY-induced lung injury (Salha et al., 2012). These anti-PLY strategies, though effective, carry several practical therapeutic difficulties. Immunisation with PLY is not an established, routine approach in patients and requires time until immunity is raised. The presence of the blood-brain and blood-CSF barrier complicates the penetration of therapeutic antibodies into the brain parenchyma and into the CSF (Gigliotti, Lee, Insel & Scheld, 1987; Neuwelt, Specht & Hill, 1986), where bacteria accumulate in meningitis. In comparison, Mg represents a well-established, inexpensive and safe alternative that has proven effective for several clinical indications over many years. Mg is used in the treatment of eclampsia (Euser & Cipolla,

2009) and as an anti-arrhythmic agent in humans, with a daily dose as high as 600 mg/kg (Moran, Gallagher, Peake, Cunningham, Salagaras & Leppard, 1995). It is also neuroprotective and anti-oedematous in traumatic brain injury (van den Heuvel & Vink, 2004), although some newer meta-analyses caution against this conclusion (Li et al., 2015). Mg lowers death, cerebral palsy and motor dysfunction in preterm infants (Crowther, Hiller, Doyle & Haslam, 2003). In cases of intra-operative ischaemia during cardiac bypass and carotid endarterectomy, Mg slows neurologic decline at 24 h postoperatively (Bhudia et al., 2006; Mack et al., 2009), but some trials fail to replicate such effects (Mathew et al., 2013). While most studies use Mg in the form of $MgSO_4$ for historical reasons, we used $MgCl_2$, which is considered to be pharmacologically comparable or even superior (Durlach, Guiet-Bara, Pages, Bac & Bara, 2005). The Mg dose applied demonstrated the well-known side effect of muscle relaxation. This needs to be considered, especially in clinical cases with depressed breathing. Muscle relaxation tends to flatten breathing movements and thus can complicate anaesthesia in animal models.

We designed several experimental paradigms of Mg treatment to identify the exact phase and mechanism of toxin/cell interaction modulated by Mg. First, we pre-treated brain tissue alone with Mg before toxin challenge, evaluating some tissue-specific effects. Changes in membrane fluidity, for example, may affect the thermodynamic barrier to membrane penetration of the toxin and thus reduce the speed of pore formation (Nagahama et al., 2007). The evidence that metal cations (including Mg) influence membrane fluidity in the brain and in platelets indeed supports such a mechanism (Ohba, Hiramatsu, Edamatsu, Mori & Mori, 1994; Sheu et al., 2002). Tissue pre-treatment with Mg alone, however, was not effective against subsequent PLY challenge, excluding to a large degree direct tissue-conditioning effects. Much more informative were our experiments with toxin pre-incubation with Mg and subsequent tissue toxin challenge in base medium conditions. Here, the effects of Mg were substantially preserved, indicating longer-lasting effects of the metal ion on the toxin molecule. Some divalent cations, such as calcium and zinc, have the capacity to inhibit the binding of PLY to membranes (Beurg et al., 2005; Franco-Vidal, Beurg, Darrouzet, Bebear, Skinner & Dulon, 2008). In contrast, Mg did not inhibit the membrane binding of PLY as assessed by Western blot analysis. Another explanation of our results points to Mg as a toxin modulator agent after membrane binding, but the electrophysiological experiments did not provide evidence for changed toxin pore properties on the single pore level, as the peaks of conductance remained unchanged.

In the mixed glial cell culture system, Mg delayed permeabilization in the first few hours after toxin challenge. At 6 h, however, lysis in all PLY-treated groups equalized. Comparative interpretation of the data from dissociated cell cultures and tissues is difficult tissues contain extracellular matrix and complex cellular composition not present in culture. The real advantage of the cell culture system, combined with live imaging, was the ability to study pore formation kinetics by PLY. There are multiple possible explanations for the delay of permeabilization by Mg: i) Mg-altered membrane turnover in the cells, or ii) Mg-affected pore assembly. The experiments involving Mg pre-treatment of slices and later addition of toxin indicated that the effects are mostly confined to the presence of toxin, supporting the second explanation. Interestingly, maintaining a high intracellular Mg concentration represents a protective mechanism against autolysis in *S. pneumoniae* (Neef, Andisi, Kim, Kuipers & Bijlsma, 2011).

Higher calcium concentrations mildly ameliorated swelling in our brain slice system (Supplementary Fig. S1C). The mechanisms involved here was most likely associated with the modulation of membrane toxin binding by calcium (Wippel et al., 2011). High calcium, however, is not an alternative to the Mg treatment due to the multiple secondary calcium-mediated effects such as enhanced cell dysfunction, excitotoxicity and accelerated cell death (Amagasa, Ogawa & Yoshimoto, 1990; Lorget et al., 2000; McGinnis, Wang & Gnegy, 1999; Ravens, Liu, Vandeplassche & Borgers, 1992), but it further confirms the critical sensitivity of the PLY molecule to divalent ions. We hypothesise that at non-lytic, pro-oedematous PLY concentrations in slices, Mg-induced delay of pore formation allows better tissue adaptation.

Pharmacologically, Mg inhibits intracellular calcium influx via endogenous calcium channels (Iseri & French, 1984) and blocks the NMDA receptors of the brain, which are involved pathogenically in multiple disease conditions. Experiments demonstrate a role of glutamate release by PLY in producing synaptic dysfunction (Wippel et al., 2013). We have shown before that the NMDA inhibition by MK-801 and AP5 does not alter the tissue swelling and astrocyte remodelling induced by PLY (Hupp et al., 2012). Indeed, Mg inhibited the decrease of PSD95 in the brains of animals with pneumococcal meningitis here, as the antagonising effect may be attributed both to the antagonised NMDA signalling and to the delayed PLY effect, but only regarding synaptic loss and not brain swelling. Apoptotic neuronal injury in meningitis (judged by active caspase-3 staining in CA2 area of the hippocampus and in the neocortex) was not significantly altered, which can be explained with the nature of the mouse model we used – all mice die without antibiotic treatment within 72

h, and some researchers consider it not sensitive enough (Liechti, Grandgirard & Leib, 2015). On the other hand, this model is more reproducible and the groups are clinically more homogenous, which allows for smaller experimental groups and more reliable statistics. The important finding here, however, was that Mg treatment prolonged the survival of infected animals without antibiotic treatment. Considering the anti-oedematous effect of Mg against PLY and the fact that brain oedema is the major cause of mortality in young adults with meningitis (Koedel, Scheld & Pfister, 2002), we believe that the enhanced survival is mostly a consequence of the reduction of brain swelling.

Calcium influx in cells in response to PLY exposure has been already demonstrated (Stringaris et al., 2002; Wippel et al., 2011). One can speculate that Mg acts as a blocker of the toxin-mediated calcium influx via pores, as it does so in multiple tissues by blocking endogenous calcium channels (Iseri & French, 1984). Here, however, we would expect certain changes in the conductance profile of PLY by Mg in black lipid membranes (even in the absence of calcium (Neuhaus & Cachelin, 1990)) that we did not observe.

In considering the therapeutic application of Mg, some authors have noted the variable pharmacological delivery of Mg to the brain (Sun, Kosugi, Kawakami, Piao, Hashimoto & Oyanagi, 2009), which does not always correspond to the serum levels after peripheral application. We suggest that this variability might explain the lack of a protective effect against PLY-induced oedema in some of the animals (3 out of 9). In the case of full-scale bacterial meningitis, however, the breakdown of the blood-brain barrier may prove useful by facilitating the delivery of Mg into the brain.

In summary, we demonstrate that Mg, a widely and safely used drug, could be an effective adjuvant therapeutic approach for pneumococcal meningitis together with other established therapies. To our knowledge, this is the first example of a clinically applicable compound that is capable of inhibiting, in therapeutic doses, the deleterious effects of a cholesterol-dependent cytolysin. Our results encourage the use of $MgCl_2$ as an adjunct to antibiotic treatment in an appropriate animal model and, when positive, followed by a clinical study in patients with bacterial meningitis.

References:

Alexander SPH, Kelly E, Marrion N, Peters JA, Benson HE, Faccenda E*, et al.* (2015). The Concise Guide to PHARMACOLOGY 2015/16: Overview. British Journal of Pharmacology 172**:** 5729-5743.

Alouf JE (2000). Cholesterol-binding cytolytic protein toxins. Int J Med Microbiol 290**:** 351-356.

Amagasa M, Ogawa A, & Yoshimoto T (1990). Effects of calcium and calcium antagonists against deprivation of glucose and oxygen in guinea pig hippocampal slices. Brain Res 526**:** 1-7.

Awad MM, Ellemor DM, Boyd RL, Emmins JJ, & Rood JI (2001). Synergistic effects of alpha-toxin and perfringolysin O in Clostridium perfringens-mediated gas gangrene. Infection and Immunity 69**:** 7904-7910.

Benz R, Ishii J, & Nakae T (1980). Determination of ion permeability through the channels made of porins from the outer membrane of Salmonella typhimurium in lipid bilayer membranes. J Membr Biol 56**:** 19-29.

Benz R, Janko K, Boos W, & Lauger P (1978). Formation of large, ion-permeable membrane channels by the matrix protein (porin) of Escherichia coli. Biochim Biophys Acta 511**:** 305-319.

Beurg M, Hafidi A, Skinner L, Cowan G, Hondarrague Y, Mitchell TJ*, et al.* (2005). The mechanism of pneumolysin-induced cochlear hair cell death in the rat. J Physiol 568**:** 211-227.

Bhudia SK, Cosgrove DM, Naugle RI, Rajeswaran J, Lam BK, Walton E*, et al.* (2006). Magnesium as a neuroprotectant in cardiac surgery: a randomized clinical trial. The Journal of thoracic and cardiovascular surgery 131**:** 853-861.

Bielecki J, Youngman P, Connelly P, & Portnoy DA (1990). Bacillus subtilis expressing a haemolysin gene from Listeria monocytogenes can grow in mammalian cells. Nature 345**:** 175-176.

Brandt CT (2010). Experimental studies of pneumococcal meningitis. Dan Med Bull 57**:** B4119.

Canvin JR, Marvin AP, Sivakumaran M, Paton JC, Boulnois GJ, Andrew PW*, et al.* (1995). The role of pneumolysin and autolysin in the pathology of pneumonia and septicemia in mice infected with a type 2 pneumococcus. J Infect Dis 172**:** 119-123.

Crowther CA, Hiller JE, Doyle LW, & Haslam RR (2003). Effect of magnesium sulfate given for neuroprotection before preterm birth: a randomized controlled trial. Jama 290**:** 2669-2676.

Douce G, Ross K, Cowan G, Ma J, & Mitchell TJ (2010). Novel mucosal vaccines generated by genetic conjugation of heterologous proteins to pneumolysin (PLY) from Streptococcus pneumoniae. Vaccine 28**:** 3231-3237.

Durlach J, Guiet-Bara A, Pages N, Bac P, & Bara M (2005). Magnesium chloride or magnesium sulfate: a genuine question. Magnes Res 18**:** 187-192.

Euser AG, & Cipolla MJ (2009). Magnesium sulfate for the treatment of eclampsia: a brief review. Stroke 40**:** 1169-1175.

Franco-Vidal V, Beurg M, Darrouzet V, Bebear JP, Skinner LJ, & Dulon D (2008). Zinc protection against pneumolysin toxicity on rat cochlear hair cells. Audiol Neurootol 13**:** 65-70.

Gerber J, Raivich G, Wellmer A, Noeske C, Kunst T, Werner A*, et al.* (2001). A mouse model of Streptococcus pneumoniae meningitis mimicking several features of human disease. Acta neuropathologica 101**:** 499-508.

Gigliotti F, Lee D, Insel RA, & Scheld WM (1987). IgG penetration into the cerebrospinal fluid in a rabbit model of meningitis. J Infect Dis 156**:** 394-398.

Grandgirard D, Burri M, Agyeman P, & Leib SL (2012). Adjunctive daptomycin attenuates brain damage and hearing loss more efficiently than rifampin in infant rat pneumococcal meningitis. Antimicrob Agents Chemother 56**:** 4289-4295.

Grandgirard D, & Leib SL (2010). Meningitis in neonates: bench to bedside. Clin Perinatol 37**:** 655-676.

Hupp S, Heimeroth V, Wippel C, Fortsch C, Ma J, Mitchell TJ*, et al.* (2012). Astrocytic tissue remodeling by the meningitis neurotoxin pneumolysin facilitates pathogen tissue penetration and produces interstitial brain edema. Glia 60**:** 137-146.

Iliev AI, Djannatian JR, Nau R, Mitchell TJ, & Wouters FS (2007a). Cholesterol-dependent actin remodeling via RhoA and Rac1 activation by the Streptococcus pneumoniae toxin pneumolysin. Proc Natl Acad Sci U S A.

Iliev AI, Djannatian JR, Nau R, Mitchell TJ, & Wouters FS (2007b). Cholesterol-dependent actin remodeling via RhoA and Rac1 activation by the Streptococcus pneumoniae toxin pneumolysin. Proc Natl Acad Sci U S A 104**:** 2897-2902.

Iliev AI, Djannatian JR, Opazo F, Gerber J, Nau R, Mitchell TJ*, et al.* (2009). Rapid microtubule bundling and stabilization by the Streptococcus pneumoniae neurotoxin pneumolysin in a cholesterol-dependent, non-lytic and Src-kinase dependent manner inhibits intracellular trafficking. Mol Microbiol 71**:** 461-477.

Iliev AI, Stringaris AK, Nau R, & Neumann H (2004). Neuronal injury mediated via stimulation of microglial toll-like receptor-9 (TLR9). Faseb J 18**:** 412-414.

Iseri LT, & French JH (1984). Magnesium: nature's physiologic calcium blocker. American heart journal 108**:** 188-193.

Jones S, & Portnoy DA (1994). Characterization of Listeria monocytogenes pathogenesis in a strain expressing perfringolysin O in place of listeriolysin O. Infection and immunity 62**:** 5608-5613.

Kastenbauer S, & Pfister HW (2003). Pneumococcal meningitis in adults: spectrum of complications and prognostic factors in a series of 87 cases. Brain 126**:** 1015-1025.

Koedel U, Scheld WM, & Pfister HW (2002). Pathogenesis and pathophysiology of pneumococcal meningitis. Lancet Infect Dis 2**:** 721-736.

Li W, Bai YA, Li YJ, Liu KG, Wang MD, Xu GZ*, et al.* (2015). Magnesium sulfate for acute traumatic brain injury. The Journal of craniofacial surgery 26**:** 393-398.

Liechti FD, Grandgirard D, & Leib SL (2015). Bacterial meningitis: insights into pathogenesis and evaluation of new treatment options: a perspective from experimental studies. Future Microbiol 10**:** 1195-1213.

Lorget F, Kamel S, Mentaverri R, Wattel A, Naassila M, Maamer M*, et al.* (2000). High extracellular calcium concentrations directly stimulate osteoclast apoptosis. Biochem Biophys Res Commun 268**:** 899-903.

Mack WJ, Kellner CP, Sahlein DH, Ducruet AF, Kim GH, Mocco J*, et al.* (2009). Intraoperative magnesium infusion during carotid endarterectomy: a double-blind placebo-controlled trial. J Neurosurg 110**:** 961-967.

Marmarou A (2007). A review of progress in understanding the pathophysiology and treatment of brain edema. Neurosurg Focus 22**:** E1.

Mathew JP, White WD, Schinderle DB, Podgoreanu MV, Berger M, Milano CA*, et al.* (2013). Intraoperative magnesium administration does not improve neurocognitive function after cardiac surgery. Stroke 44**:** 3407-3413.

McGinnis KM, Wang KK, & Gnegy ME (1999). Alterations of extracellular calcium elicit selective modes of cell death and protease activation in SH-SY5Y human neuroblastoma cells. J Neurochem 72**:** 1853-1863.

Moran JL, Gallagher J, Peake SL, Cunningham DN, Salagaras M, & Leppard P (1995). Parenteral magnesium sulfate versus amiodarone in the therapy of atrial tachyarrhythmias: a prospective, randomized study. Crit Care Med 23**:** 1816-1824.

Nagahama M, Otsuka A, Oda M, Singh RK, Ziora ZM, Imagawa H*, et al.* (2007). Effect of unsaturated bonds in the sn-2 acyl chain of phosphatidylcholine on the membrane-damaging action of Clostridium perfringens alpha-toxin toward liposomes. Biochim Biophys Acta 1768**:** 2940-2945.

Nau R, Wellmer A, Soto A, Koch K, Schneider O, Schmidt H*, et al.* (1999). Rifampin reduces early mortality in experimental Streptococcus pneumoniae meningitis. J Infect Dis 179**:** 1557-1560.

Neef J, Andisi VF, Kim KS, Kuipers OP, & Bijlsma JJ (2011). Deletion of a cation transporter promotes lysis in Streptococcus pneumoniae. Infect Immun 79**:** 2314-2323.

Neuhaus R, & Cachelin AB (1990). Changes in the conductance of the neuronal nicotinic acetylcholine receptor channel induced by magnesium. Proceedings Biological sciences / The Royal Society 241**:** 78-84.

Neuwelt EA, Specht HD, & Hill SA (1986). Permeability of human brain tumor to 99mTc-gluco-heptonate and 99mTc-albumin. Implications for monoclonal antibody therapy. Journal of neurosurgery 65**:** 194-198.

O'Hara J (2008). How I do it: sample size calculations. Clinical otolaryngology : official journal of ENT-UK ; official journal of Netherlands Society for Oto-Rhino-Laryngology & Cervico-Facial Surgery 33**:** 145-149.

Ohba S, Hiramatsu M, Edamatsu R, Mori I, & Mori A (1994). Metal ions affect neuronal membrane fluidity of rat cerebral cortex. Neurochem Res 19**:** 237-241.

Paton JC, Lock RA, & Hansman DJ (1983). Effect of immunization with pneumolysin on survival time of mice challenged with Streptococcus pneumoniae. Infection and Immunity 40**:** 548-552.

Raslan A, & Bhardwaj A (2007). Medical management of cerebral edema. Neurosurg Focus 22**:** E12.

Ravens U, Liu GS, Vandeplassche G, & Borgers M (1992). Protection of human, rat, and guinea-pig atrial muscle by mioflazine, lidoflazine, and verapamil against the destructive effects of high concentrations of Ca2+. Cardiovasc Drugs Ther 6**:** 47-58.

Reiß A, Braun JS, Jäger K, Freyer D, Laube G, Bührer C*, et al.* (2011). Bacterial Pore-Forming Cytolysins Induce Neuronal Damage in a Rat Model of Neonatal Meningitis. Journal of Infectious Diseases 203**:** 393-400.

Salha D, Szeto J, Myers L, Claus C, Sheung A, Tang M*, et al.* (2012). Neutralizing antibodies elicited by a novel detoxified pneumolysin derivative, PlyD1, provide protection against both pneumococcal infection and lung injury. Infection and Immunity 80**:** 2212-2220.

Sheu JR, Hsiao G, Shen MY, Fong TH, Chen YW, Lin CH*, et al.* (2002). Mechanisms involved in the antiplatelet activity of magnesium in human platelets. Br J Haematol 119**:** 1033-1041.

Southan C, Sharman JL, Benson HE, Faccenda E, Pawson AJ, Alexander S P H*, et al.* (2016). The IUPHAR/BPS Guide to PHARMACOLOGY in 2016: towards curated quantitative interactions between 1300 protein targets and 6000 ligands. Nucleic Acids Research 44**:** D1054-1068.

Spreer A, Kerstan H, Bottcher T, Gerber J, Siemer A, Zysk G*, et al.* (2003). Reduced release of pneumolysin by Streptococcus pneumoniae in vitro and in vivo after treatment with nonbacteriolytic antibiotics in comparison to ceftriaxone. Antimicrob Agents Chemother 47**:** 2649-2654.

Stamatovic SM, Dimitrijevic OB, Keep RF, & Andjelkovic AV (2006). Inflammation and brain edema: new insights into the role of chemokines and their receptors. Acta Neurochir Suppl 96**:** 444-450.

Stringaris AK, Geisenhainer J, Bergmann F, Balshusemann C, Lee U, Zysk G*, et al.* (2002). Neurotoxicity of pneumolysin, a major pneumococcal virulence factor, involves calcium influx and depends on activation of p38 mitogen-activated protein kinase. Neurobiol Dis 11**:** 355-368.

Sun L, Kosugi Y, Kawakami E, Piao YS, Hashimoto T, & Oyanagi K (2009). Magnesium concentration in the cerebrospinal fluid of mice and its response to changes in serum magnesium concentration. Magnes Res 22**:** 266-272.

Tengvar C, Forssen M, Hultstrom D, Olsson Y, Pertoft H, & Pettersson A (1982). Measurement of edema in the nervous system. Use of Percoll density gradients for determination of specific gravity in cerebral cortex and white matter under normal conditions and in experimental cytotoxic brain edema. Acta Neuropathol 57**:** 143-150.

Tilley SJ, Orlova EV, Gilbert RJ, Andrew PW, & Saibil HR (2005). Structural basis of pore formation by the bacterial toxin pneumolysin. Cell 121**:** 247-256.

van den Heuvel C, & Vink R (2004). The role of magnesium in traumatic brain injury. Clin Calcium 14**:** 9-14.
Wall EC, Gordon SB, Hussain S, Goonetilleke UR, Gritzfeld J, Scarborough M*, et al.* (2012). Persistence of Pneumolysin in the Cerebrospinal Fluid of Patients With Pneumococcal Meningitis Is Associated With Mortality. Clinical infectious diseases 54**:** 701-705.

Wellmer A, Zysk G, Gerber J, Kunst T, Von Mering M, Bunkowski S*, et al.* (2002). Decreased virulence of a pneumolysin-deficient strain of Streptococcus pneumoniae in murine meningitis. Infect Immun 70**:** 6504-6508.

Wippel C, Fortsch C, Hupp S, Maier E, Benz R, Ma J*, et al.* (2011). Extracellular calcium reduction strongly increases the lytic capacity of pneumolysin from streptococcus pneumoniae in brain tissue. J Infect Dis 204**:** 930-936.

Wippel C, Maurer J, Förtsch C, Hupp S, Bohl A, Ma J*, et al.* (2013). Bacterial Cytolysin during Meningitis Disrupts the Regulation of Glutamate in the Brain, Leading to Synaptic Damage. PLoS Pathog 9**:** e1003380.
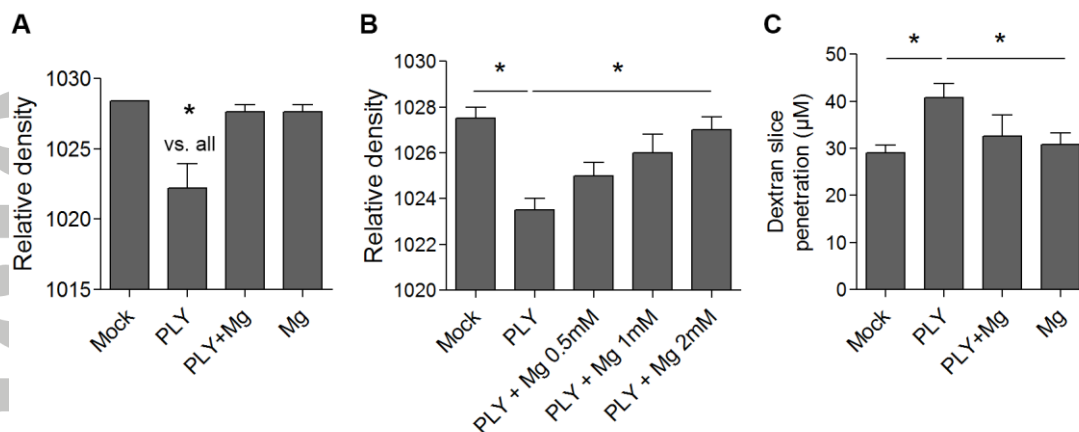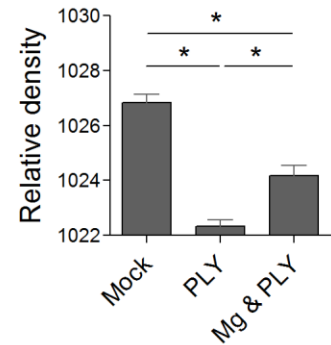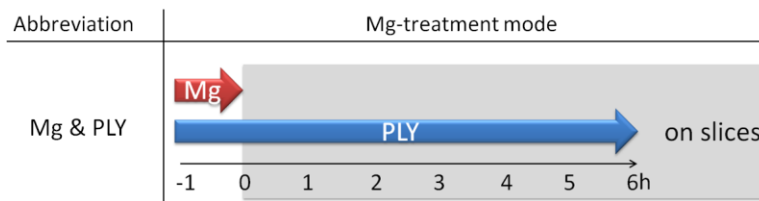
Figure 1. Ex vivo inhibition of PLY-induced swelling by magnesium chloride (Mg). *A*. Relative density (lower density indicates higher water content and swelling) of brain slices after 6 h incubation without treatment (mock), with exposure to 4 HU/ml PLY (PLY), treatment with 2 mM Mg only (Mg) or combined exposure to PLY and Mg (n=6 independent experiments). *B*. Mg dose-dependent inhibition of rat brain swelling after 6 h co-exposure of 4 HU/ml PLY (n=5 independent experiments). *C*. Effect of 2 mM Mg to 4 HU/ml PLY on penetration of dextran-TRITC in rat brain slices (n=5 independent experiments).
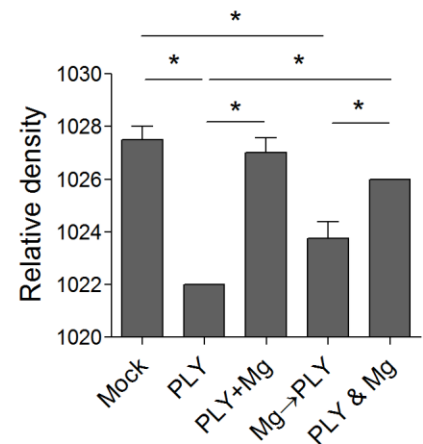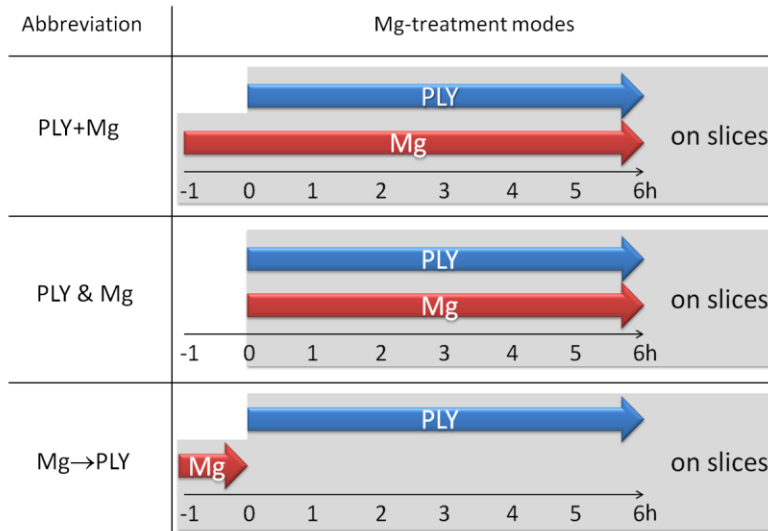
Figure 2. Attenuation of brain swelling by different Mg application schedules. *A*. Schematic diagram of the different modes of Mg application (left). Inhibition of PLY-induced oedema by 4 HU/ml for 6 h by simultaneous incubation with 2 mM Mg with 1 h Mg pre-incubation of the slices (PLY+Mg) and without slice pre-incubation (PLY & Mg). Pre-incubation of the slices with Mg for 1 h and removal before adding PLY (Mg→PLY) did not alter toxin-triggered oedema (n=5 independent experiments). *B*. Partial inhibition of rat brain slice swelling by pre-incubation of PLY with 2 mM Mg for 1 h, followed by treatment of slices in normal medium without extra Mg with 4 HU/ml PLY for 6 h (n=5 independent experiments).
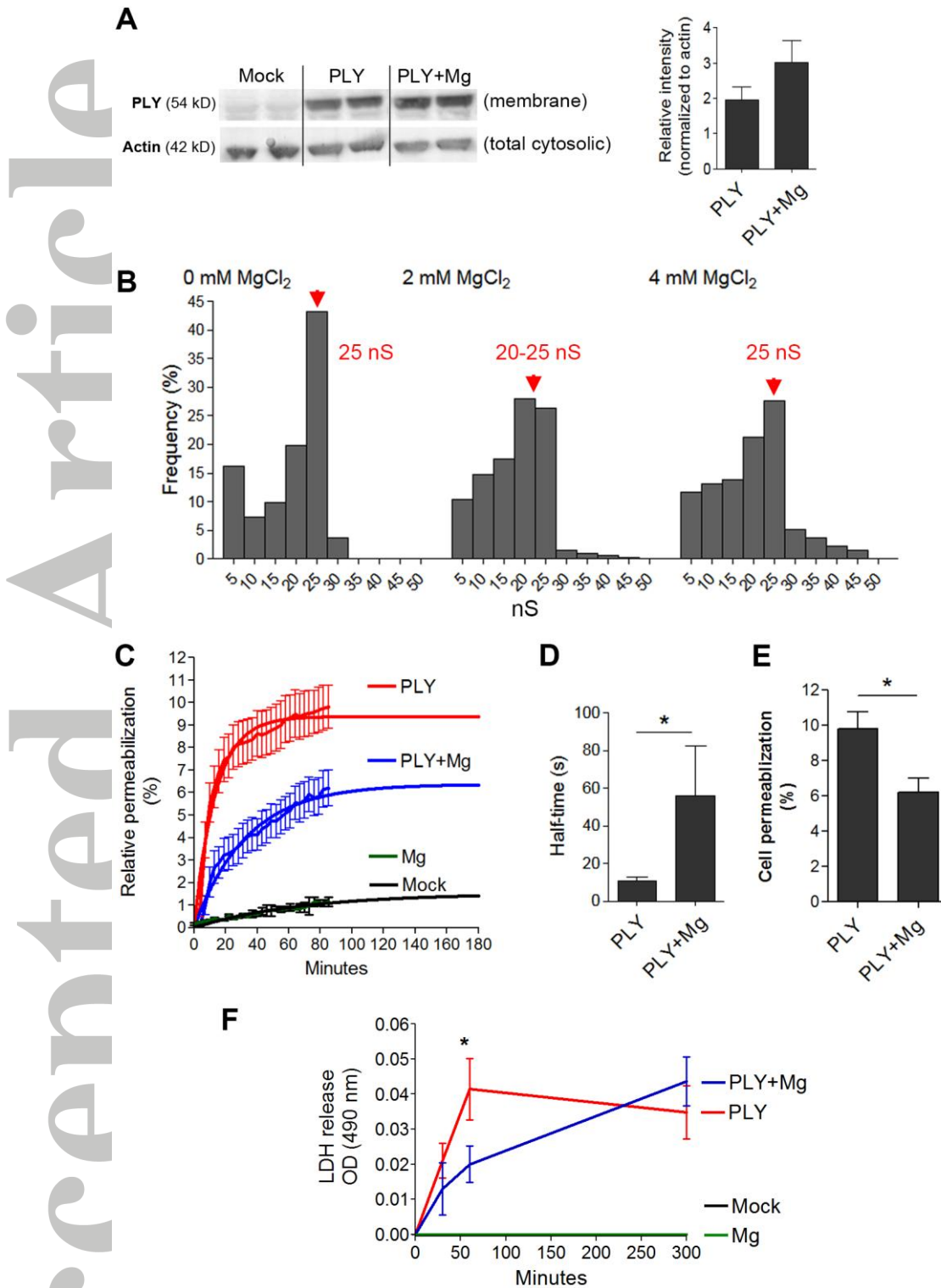
Figure 3. Mechanisms of modulation of PLY properties by Mg. *A*. The presence of Mg does not inhibit toxin binding to mouse glial cells (Western blot) 15 min after challenge with 4 HU/ml (4 independent experiments). *B*. The conductance profile of PLY in a black lipid bilayer demonstrates an unchanged conductance pattern that is independent of the Mg concentration. The number of measured events is as follows: mock – 130 events, 2 mM Mg –

330 events, 4 mM – 127 events with peak conductance for mock at 25 nS, for 2 mM Mg at 20-25 nS and for 4 mM Mg at 25 nS. *C*. Live-cell imaging analysis of mouse glial cell membrane permeabilisation (as judged by propidium iodide (PI) staining) by 4 HU/ml PLY reveals delayed permeabilisation and diminished number of permeabilised cells during treatment with 2 mM Mg. The curves are extrapolated beyond 120 min using non-linear regression curves fitted with one-phase exponential association (n=5 independent experiments). *D*. Increased half-time of PLY permeabilisation during treatment with 2 mM Mg (n=5 independent experiments). *E*. Diminished permeabilisation at the plateau of the regression curve in the presence of 2 mM Mg treatment (n=5 independent experiments). *F*. Diminished LDH release by Mg at 60 min after PLY challenge, followed by equalized release at 6 h (n=5 independent experiments).
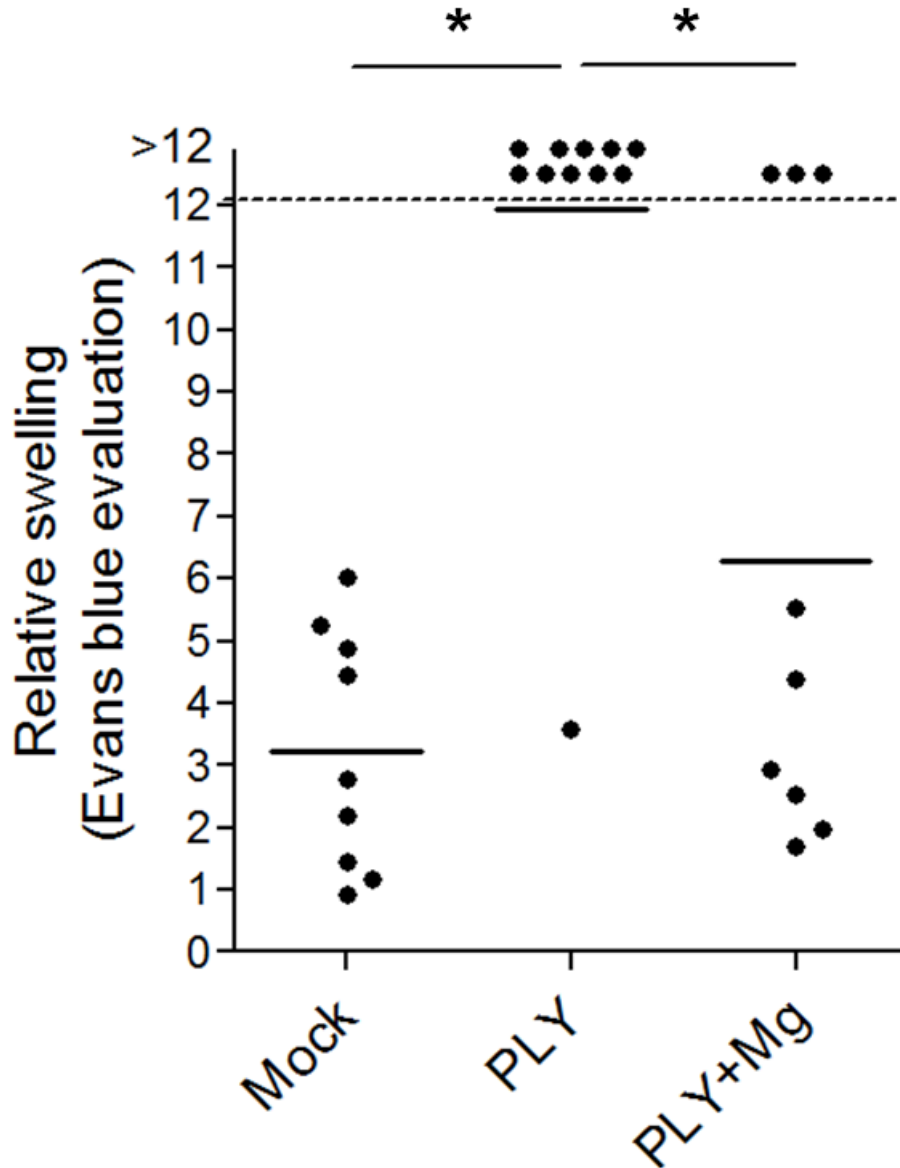
Figure 4. Effect of Mg on PLY brain oedema model in infant rats. The amount of Evans Blue (expressed as mm^2 after filter paper absorption) displaced out of the intracranial space (as a marker of elevated intracranial pressure) at 6 h after treatment with PLY (see Methods) in rats with or without 500 mg/kg ip MgCl$_2$ application at the beginning of the experiment reveals ameliorated intracranial pressure increase by Mg. The intracranial pressure of the PLY-treated animals is significantly higher compared with the mock and PLY+Mg groups. Graph presents mean as well.
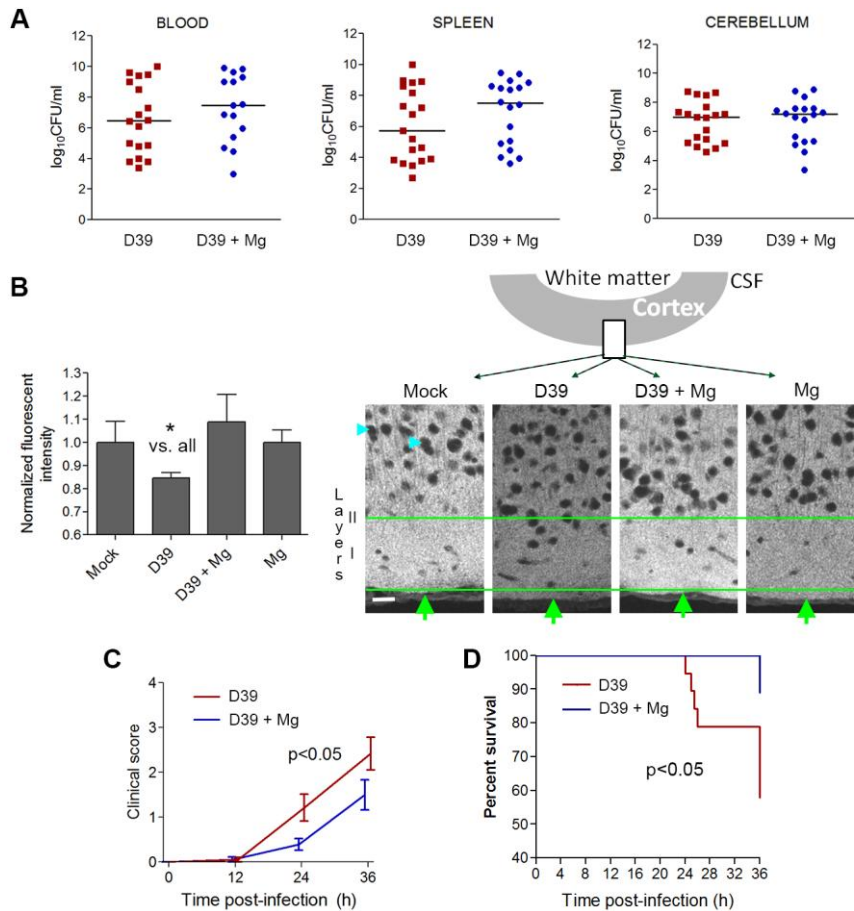
Figure 5. Effect of Mg treatment in mice with experimental *S. pneumoniae* D39 meningitis. *A*. *S. pneumoniae* D39 concentrations (as colony-forming units, CFU) in blood, cerebellum and spleen homogenates after 36 h demonstrated comparable growth in infected mice treated ip with 0.45% NaCl (Mock) or treated ip with $MgCl_2$ (Mg). *B*. Relative fluorescent intensity measurement of the PSD95 immunofluorescence in layers 1-3 of the neocortex at the level of the postcentral gyrus (Mock (n=4 animals): NaCl-injected and NaCl-treated group; D39 (n=19 animals): Spn D39-infected and NaCl-treated group; D39 + Mg (n=18 animals): Spn D39-infected and $MgCl_2$-treated group; Mg (n=3 animals): NaCl-injected and $MgCl_2$-treated group) and corresponding fluorescent images (cyan arrows indicate staining-negative nuclear regions; green arrows – cortical surface; green lines limit the region of interest, including layer I and partially layer II; schematic diagram above indicates the position of the imaged fragment). Scale bar: 20 μm. *C*. Clinical score (0 = no apparent behavioural abnormality; 1, moderate lethargy; 2 = severe lethargy; 3 = unable to walk; 4 = dead) of the animals. Mock and Mg controls demonstrate score of 0 (not included in the graph, overlap with axis). For statistical analysis, the area under the curve is calculated and compared (see Methods). *D*. Survival curves of $MgCl_2$ (Mg, n=18) or NaCl-treated

(Mock, n=19) infected animals. All mock and Mg controls demonstrate 100% survival at 36 h (not included in the graph, overlap of multiple lines).

List of Hyperlinks for Crosschecking

Magnesium -
http://www.guidetopharmacology.org/GRAC/LigandDisplayForward?ligandId=708